Supporting Information

Effects of Silver Nanoparticles with Different Sizes on Photochemical Responses of Polythiophene-fullerene Thin Films

Jing You, [a] Kwati Leonard,[a] Yukina Takahashi, [a,b] Hiroaki Yonemura, [a,b] and Sunao Yamada*[a,b]

[a] Department of Applied Chemistry, Faculty of Engineering, Kyushu University,744 Moto-oka, Nishi-ku, Fukuoka, Japan. Fax: +81-92-802-2815; Tel: +81-92-802-2812; E-mail: yamada@mail.cstm.kyushu-u.ac.jp

[b] Center for Future Chemistry, Kyushu University, 744 Moto-oka, Nishi-ku, Fukuoka, Japan.

1. Size distribution of AgPs

Size distribution of 64- and 7-nm AgPs were evaluated from TEM observation as shown in Fig. S1

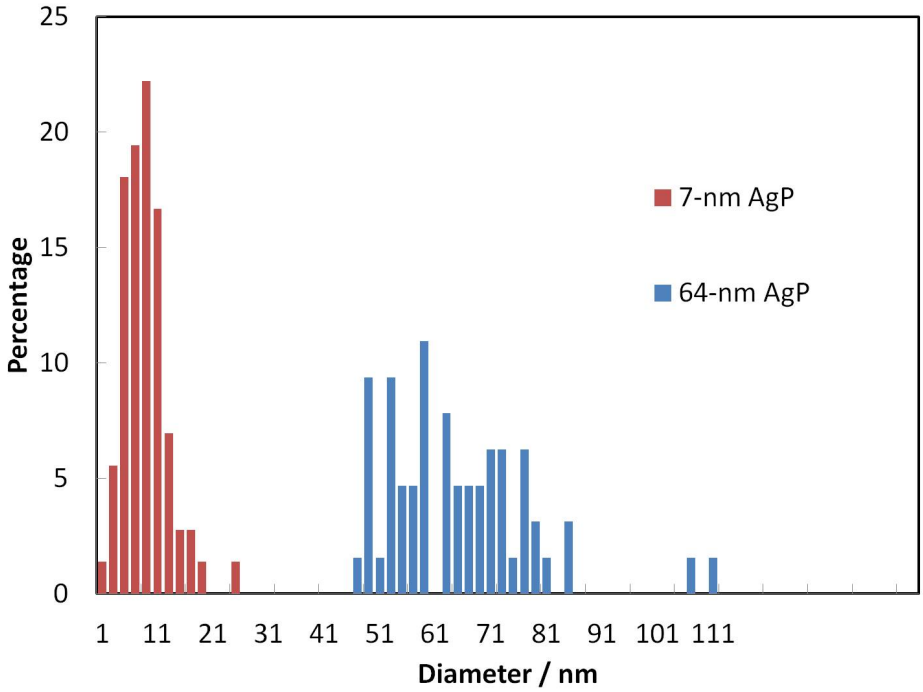

Fig. S1 Size distribution of AgPs.

2. Estimation of P3HT:PCBM film thickness

The data of absorption spectra and thicknesses of P3HT:PCBM films has been published in ref. 17. This relationship is shown in Fig. S2.

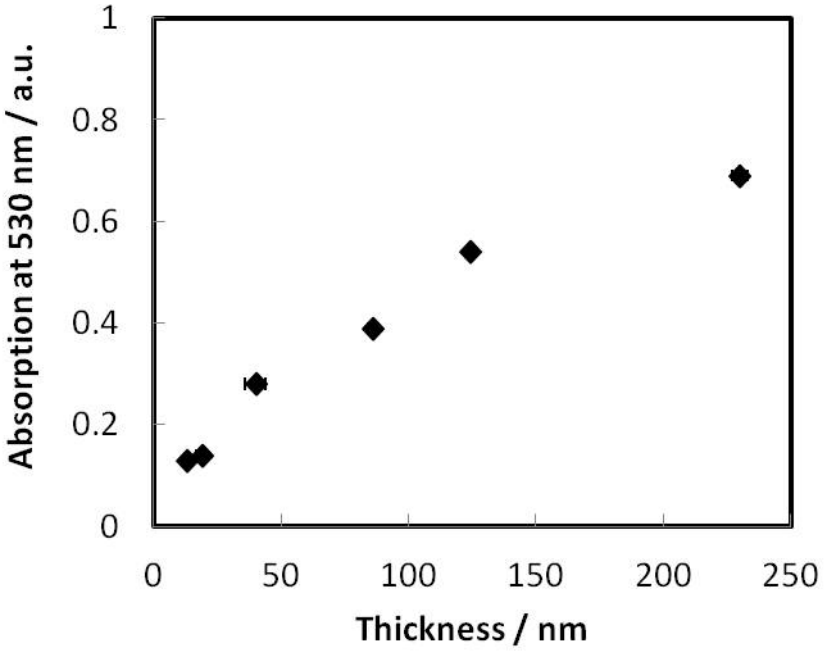

Fig. S2 Absorption at 530 nm as function of P3HT:PCBM thickness.

From Fig. S2, we can see that the absorption peak intensity of P3HT:PCBM film at 530 nm was increased linearly with increasing film thickness. As shown in the Fig. 8 (A), the absorption of P3HT:PCBM film without AgPs at 530 nm was ~ 0.5-0.6. Thus, the thickness was in the region of 100-130 nm, judging from Fig. S2.

3. Absorption spectra of P3HT films in the presence of deposited AgPs with different coverage density.

Extinction spectra of the samples with different AgPs densities are shown in Fig. S3.

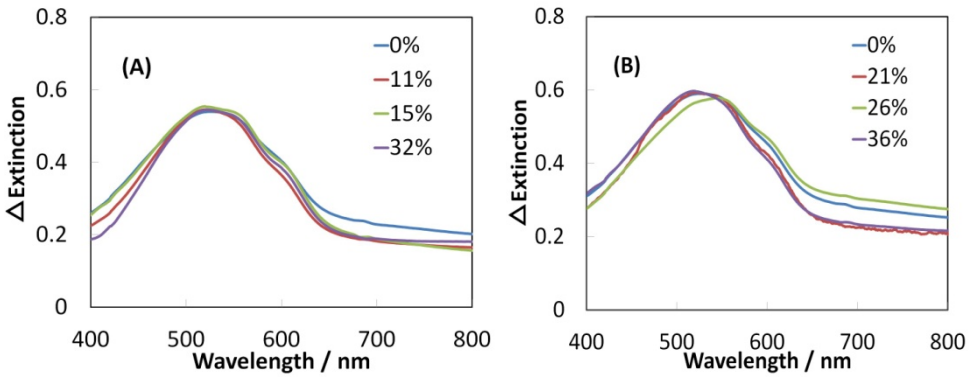

Fig. S3: Extinction spectra of P3HT layer in the presence of (A) 64-nm (B) 7-nm AgPs with

different densities.

As shown in Fig. S3 (A) and (B), the extinction spectra of P3HT layer are roughly same. It indicates that the thickness and structure of P3HT layer are roughly same even with different coverage densities of deposited AgPs. The enhancement of fluorescence is mainly due to the presence of AgPs.

4. Mechanism of formation of nanoplate or nanoprism with aggregated 7-nm AgPs.

SEM images of 7-nm AgPs shown in Fig. 4 (D), (E), (F) were scaled directly from the respective images in Fig. S4 as shown below:

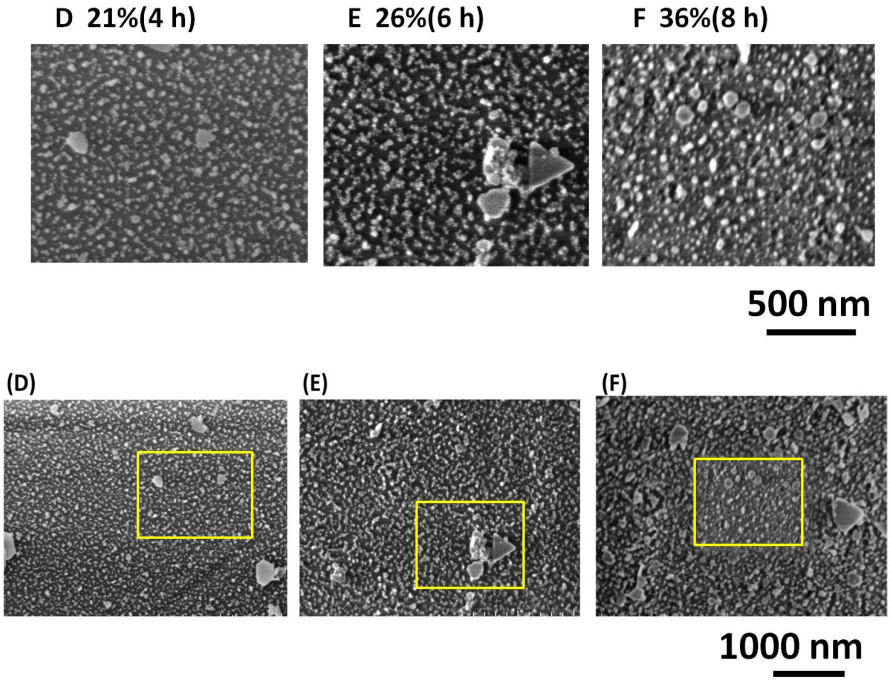

Fig. S4 SEM images of 7-nm AgPs with scale of 1000 nm

The brief description of formation process is as follow: in the presence of oxygen, the plasmonic excitation of AgPs (< 10 nm) will slowly generate Ag^+ in the bulk. Then, Ag^+ will be reduced again in the presence of citrate ions, and turn into Ag to form nanoprism and/or plates, as has been described previously.[1-4]

In the case of 7-nm AgPs, as shown in Fig. 4(D), when the immersion time was ~ 4 h, most of AgPs were well dispersed and only small size and quantity of nanoprism and/or plate formed. With increasing immersion time, nanoprisms and/or plates become larger and quantity was also increased (Fig. 4(E) and (F). When the immersion time ~ 8 h (Fig. 4(F)) except formed more nanoprisms and/or plates, the quantity of isolated AgPs was also decreased. This process is agreed with the formation process described in ref. 1-4.

5. Decrease of scattering efficiency after fusion.

The scattering efficiencies of aggregated 7-nm AgPs before and after fusion were simulated using DDA method. Models are shown in Fig. S5. The refractive index of silver is from ref. 5.

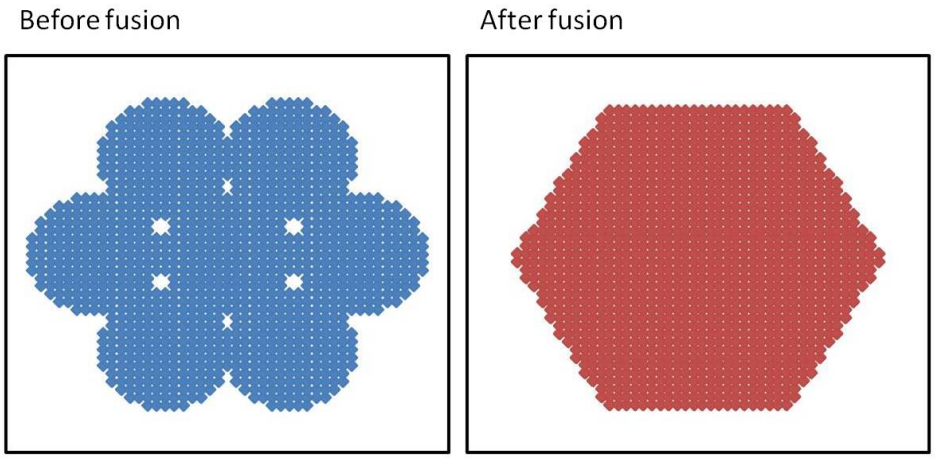

Fig. S5 Simulation models

As shown in Fig. S5, seven contacted spheres were used to denote the aggregated 7-nm AgPs. Whereas, a hexagonal prism was used to denote the nanoplate generated from coalescence of aggregated AgPs. Here, we set the 1791 dipole to denote one Ag-sphere. The diameter of one Ag-sphere was denoted by 15 dipoles. Similarly, the height of hexagonal prism was 15 dipoles. The hexagonal prism has same dipoles and same physical volume as 7 contact spheres. The simulation was from 300 nm to 890 nm. Results are shown in Fig. S6.

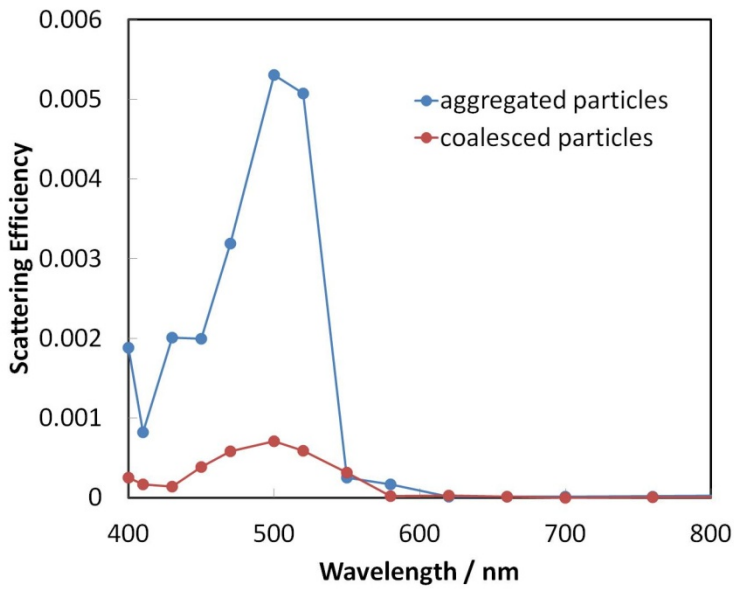

Fig. S6 DDA simulation of scattering efficiency of aggregated 7-nm AgPs and coalescing nano-plate with same volume.

As shown in Fig.S6, with same volume, the scattering efficiency of aggregated 7-nm AgP sphere was more than 5 times larger than nanoplate generated from coalescence.

6. Detail of DDA simulation of scattering efficiency of ITO/AgP(20%)/P3HT.

The refractive index of silver, ITO and P3HT were obtained from ref. 5, 6 and 7, respectively. In the case of 64-nm AgPs, more than 9 times larger than 7 nm AgPs for diameter, we use 389 dipoles (diameter = 9 dipoles) to denote one 64-nm AgP, 1 dipole equal to 7.1 nm for calculation convenience and limitation. In this case, the cross section of 64-nm AgP was denoted by 69 dipoles. The area of ITO surface was denoted by 69×25/0.2 = 8625 dipoles, and the physical area of ITO is 4.348×10^5 nm^2. The thickness of ITO is about 100 nm. The volume of ITO was denoted by 120750 dipoles. Similarly, 100-nm P3HT layer with the same area was also denoted by 120750 dipoles. The total dipoles used in this mode are 241500 and the physical volume of this ITO/AgP/P3HT block deposited 64-nm AgPs is 4.348×10^7 nm^3. The distribution of 64-nm AgPs on the ITO is shown in Fig. S7 (A).

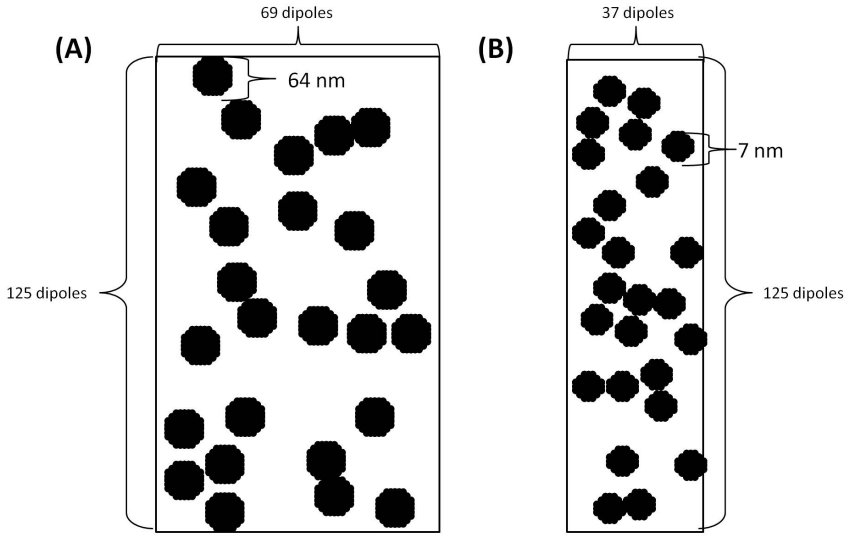

Fig. S7 Distribution of 25 AgPs on ITO surface with the density of 20%, (64-nm AgPs(A); 7-nm AgPs(B))

In the case of 7-nm AgPs, we use 179 dipoles (diameter = 7 dipoles) to denote one 7-nm AgP, where 1 dipole is equal to 1 nm. In this case, the cross section of 7-nm AgP was denoted by 37 dipoles. We also assumed 25 deposited AgPs on the ITO surface with the density of 20%. The area of ITO surface was denoted by 37×25/0.2 = 4625 dipoles, and the area of ITO is 4.625×10^3 nm^2. The thickness of ITO is about 100 nm, and the volume of ITO was denoted by 462500 dipoles. Similarly, 100-nm P3HT layer with the same area was also denoted by 462500 dipoles. The total dipoles used in this mode are 925000 and the physical volume of this ITO/AgP/P3HT block was 9.25×10^5 nm^3. The distribution of AgPs on the ITO is shown in Fig. S7 (B).

As described above, with the same number of deposited AgPs on ITO surface, the physical volume of ITO/AgP/P3HT with 64-nm AgPs is much larger than the case of 7-nm. While, sample areas for all the measurements were same. So, we used the periodic method of DDA simulation to investigate the extinction and scattering properties.[7] The area of one ITO/AgP/P3HT with 64-nm AgPs, as shown in Fig. S7(A), is equal to 91 times of area of ITO/AgP/P3HT in the case of 7-nm AgPs. The relationship between extinction efficiency and differential extinction cross section (dC_{ext}/dA) in periodic structure is:

$$\frac{dC_{ext}}{dA} = \frac{Q_{ext}\alpha_{eff}^2}{L_x L_y}$$

Here, Q_{ext} is the extinction efficiency of one block. α_{eff} the effective radius defined by $\alpha_{eff} = [3\times V/(4\times\pi)]^{1/3}$. L_x the repeating unit in the x direction, and L_y in the y direction.[5] In the case of 64-nm AgPs, we set the ITO/AgP/P3HT without repeating in the x and y direction. In order to get same physical volume as the case of 64-nm, in the case of 7-nm AgPs, it repeated 13 times in the x direction, and 7 times in the y direction. The physical volume V is 9.25×10^5 nm^3. It is same as in the case of $Q_{sca.}$

Extinction efficiency spectra from DDA simulation and experimental obtained extinction spectra are shown in the Fig. S8.

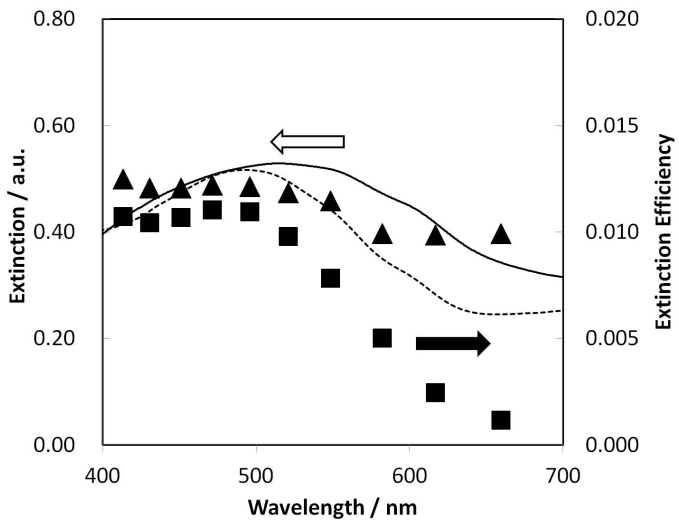

Fig. S8 Extinction spectra of ITO/AgP/P3HT with deposited 64-nm AgPs (solid line) and 7-nm AgPs (dotted line); Differential extinction cross section of ITO/AgP/P3HT with deposited 64-nm AgPs (solid triangle) and 7-nm AgPs (solid square).

From the Fig. S8, the deposited 64-nm AgPs showed larger enhancement of extinction at the region of 600-700 nm as compared with 7-nm AgPs, which corresponded to the plasmon band of coupled or aggregated AgPs. It is clear that the simulation result agrees with the

experimental results. This simulation can be applied to investigate the percentage of scattering in extinction for the sample with the structure of ITO/AgP/P3HT 64- and 7- nm diameters.

1. R. C. Jin, Y. W. Cao, C. A. Mirkin, K. L. Kelly, G. C. Schatz, and J. G. Zheng, *Science*, 2001, **294**, 1901.
2. X. Wu, P. L. Redmond, H. Liu, Y. Chen, M. Steigerwald, and L. Brus, *J. Am. Chem. Soc.,* 2008, **130**, 9500.
3. P. L. Redmond, X. Wu, and L. Brus. *J. Phys. Chem. C,* 2007, **111**, 8942.
4. G. P. Lee, Y. Shi, E. Lavoie, T. Daeneke, P. Reineck, U. B. Cappel, D. M. Huang, and U. Bach, *ACS Nano,* 2013, **7**, 5911."
5. B. T. Draine, P. J. Flatau, *J. Opt. Soc. Am. A*, 1994, **11**, 1491.
6. H. Wormeester, F. Monestier, J. J. Simon, P. Torchio, L. Escoubas, F. Flory, S. Bailly, R. de Bettignies, S. Guillerez, and C. Defranoux, *Sol. Energy Mater. Sol. Cells*, 2007, **91**, 405.
7. B. T. Draine, P. J. Flatau, *J. Opt. Soc. Am. A,* 2008, **25**, 2693.